10.24425/acs.2023.146280

Archives of Control Sciences
Volume 33(LXIX), 2023
No. 2*, pages 371–390*

Real-time validation of an automatic generation control system considering HPA-ISE with crow search algorithm optimized cascade FOPDN-FOPIDN controller

Naladi Ram BABU, Tirumalasetty CHIRANJEEVI, Ramesh DEVARAPALLI, Łukasz KNYPIŃSKI and Fausto Pedro GARCÍA MÁRQUEZ

This article validates the application of RT-Lab for the AGC studies of three-area systems. All the areas are employed with thermal-DSTS systems. A new controller named cascade FOPDN-FOPPIDN is employed. Its parameters are optimized using a CSA, subjecting to a new PI named HPA-ISE. The responses of the FOPDN-FOPIDN controller are related and are superior over PIDN and TIDN controllers. Moreover, the dominance of HPA-ISE is verified with ISE, and it performs better in terms of system dynamics. Further, the system performance reliability is analyzed with the AC-HVDC and is better than the AC system. Besides, sensitivity analysis recommends that the proposed FOPDN-FOPIDN at diverse conditions is robust and more reliability.

Key words: crow search algorithm, dish-stirling solar system, AGC, RT Lab, FOPDN-FOPIDN controller

N.R. Babu (e-mail: rambabu.nits@yahoo.com) is with Department of Electrical and Electronics Engineering, Aditya Engineering College, Surampalem, Andhra Pradesh, India.

T. Chiranjeevi (e-mail: tirumalasetty.chiranjeevi@recsonbhadra.ac.in) is with Department of Electrical Engineering, Rajkiya Engineering College Sonbhadra, U.P., India.

R. Devarapalli (e-mail: Dr.R.Devarapalli@gmail.com) is with Department of Electrical/Electronics and Instrumentation Engineering, Institute of Chemical Technology, Indianoil Odisha Campus, Bhubaneswar 751013, India.

Ł. Knypiński (e-mail: lukasz.knypinski@put.poznan.pl) is with Faculty of Control, Robotics and Electrical Engineering, Poznan University of Technology Piotrowo 3A, 60-965 Poznań, Poland.

F.P. García Márquez (corresponding author, e-mail: FaustoPedro.Garcia@uclm.es) is with Ingenium Research Group, University of Castilla-La Mancha, Spain.

The work reported herein was supported financially by the Ministerio de Ciencia e Innovación (Spain) and the European Regional Development Fund, under the Research Grant WindSound project (Reference: PID2021-125278OB-I00).

Received 21.6.2022.

1. Introduction

AGC aims to shrink the disparity amid generation and load [1]. This disparity violation rises to frequency and power abnormalities. If these mismatch persist for long time, it leads to damage and is overcome by AGC. AGC works commenced thru one [2] and prolonged to multi-area systems [3]. Realistic systems are developed by considering generation rate constraint (GRC) and droop. AGC studies with Thermal-hydro, Thermal-Gas with GRC and GDB are presented in [4, 5].

Fossil fuels are the main source for electricity generation. But the excess carbon emission by hampering the environment tend to contribute to the renewable energy source (RES) penetration. Wind and solar energy dominate over other renewable. Bevrani et al. [6] integrated the photovoltaic system in AGC study. Das et al. [7] proposed an AGC study comprising solar thermal power plants (STPPs). The idea of integrating DSTS and wind units in AGC studies are proposed by Rahman [8, 9]. Also, the AGC studies in [10–12] presented the renewable energy source (RES) integration of wind, DSTSs and STPPs of two-area systems only. Also, only a few literatures mentioned the use of Solar. Thus, AGC research with multiple solar (DSTS) units with thermal provides opportunity.

System dynamics can be weakened in abnormal circumstances. Also, increased load demand tends to enhance the inter-area power transfer capability. Therefore, HVDC is connected across AC link. During the exchange of spinning reserves among inter-areas, HVDC suppress cascading outages and helps in power flow. Also, transient presence in transmission lines would exacerbate the system dynamics and it can be exterminated by incorporating HVDC [13, 14]. AGC system with HVDC are studied by Sharma et al. [15–17]. Rakhshani et al. [14] and Pathak et al. [18] demonstrated the AGC study considering integral and derivative control in the two-area system. Further, the AGC-HVDC studies did not involve RES integration like DSTSs in all areas that need further investigation.

In present days, AGC research focuses on the strategy of ancillary controllers, which contribute to restoring the system indices to nominal values. Controllers like integer orders (IO-PIDN) [19], fractional orders (FOPID) [20], tilt (TID) control [21], and the integer-FO cascade controllers [8] are studied. FO controllers surpass IO controllers by providing flexibility with more tuning parameters. Further, the authors proposed a cascade combination of IO-FO controllers [10]. Authors in [22, 23] presented two FO cascade controllers. Also, various cascade amalgamations of two FO controllers may produce superior dynamics. A new cascade combination of FOPDN-FOPIDN is proposed for AGC research which offers wide study.

Controller parameter optimization leads to optimum solutions and can be attained by evolutionary algorithms (EA). EAs like whale [10], sine-cosine [11], firefly [19], cuckoo search [24], spider monkey [25], Harris hawk's with particle swarm [26], biogeography [27], coyote optimization [28] etc., are presented. A latest EA named crow-search algorithm (CSA) [29, 30] is handy, it is based on the crow's food-finding behaviour. The properties of food search, face recognition, tools' usage, communication methods, and greedy nature make the crow a clever bird. This offers further assessments.

The above AGC research is implemented in MATLAB software. However, the validation of AGC studies in a RT-Lab is not carried. This calls for further investigations. The aims are as follows, based on the above-mentioned literature:

a) To model an unequal three thermal area system with DSTS and HVDC.
b) To perform an assessment with the suggested FOPDN-FOPIDN controller over PID and TID.
c) To apply the CSA algorithm for controller optimization
d) To execute SA and to check the reliability of the FOPDN-FOPIDN controller.
e) To apply the AC-HVDC system.
f) To validate the obtained results in RT-Lab software.

2. System investigated

The three thermal area system with 1:2:3 as capacity ratio considering drop and GRC is combined with HVDC and DSTS. The power expression for AC-HVDC with gain (K) and time constant (T) is given by Eq. (1).

$$\Delta P_{\text{tie}\,ij} = \left(\frac{2\pi T_{jk}}{s} + \frac{K_{DC}}{1 + sT_{DC}}\right)\left(\Delta F_j - \Delta F_k\right), \tag{1}$$

Investigation are carried for (a) thermal systems in MATLAB, (b) systems-(i) with RT-Lab application, (c) thermal-DSTS systems with RT-Lab application and (d) systems-(iii) with HVDC integration. The study system is in Fig. 1 and its transfer function (TF) model of the studied system employing the FOPDN-FOPIDN controller that is shown in Fig. 2. Controllers like PIDN, TIDN and proposed FOPDN-FOPIDN are considered with 1% SLP in area-1. Nominal parameters are noted in the Section Notations. The controller parameters are optimized by CSA with HPA-ISE are given by Eq. (2).

$$\eta_{\text{HPA-ISE}} = \int_0^t \left\{\Delta F_j^2 + \Delta F_{j-k}^2 + \left|\Delta F_{j,\text{peak}}\right| + \left|\Delta F_{j-k,\text{peak}}\right|\right\} \mathrm{d}t, \tag{2}$$

where the area numbers (j, k and m).

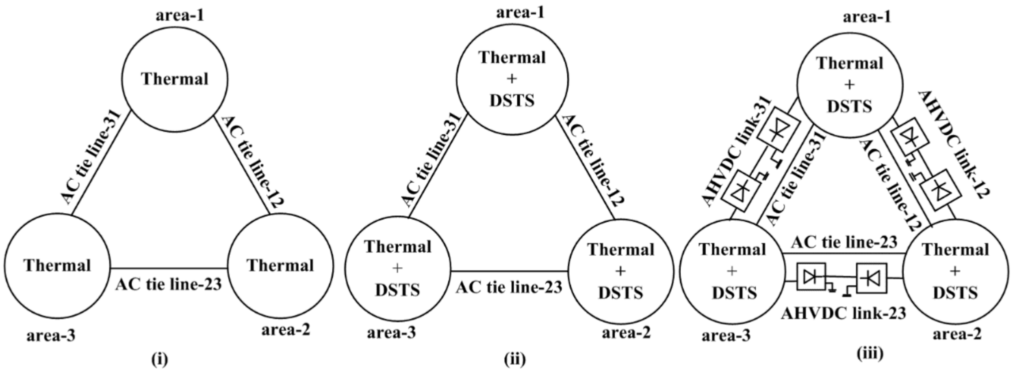

Figure 1: The study system model

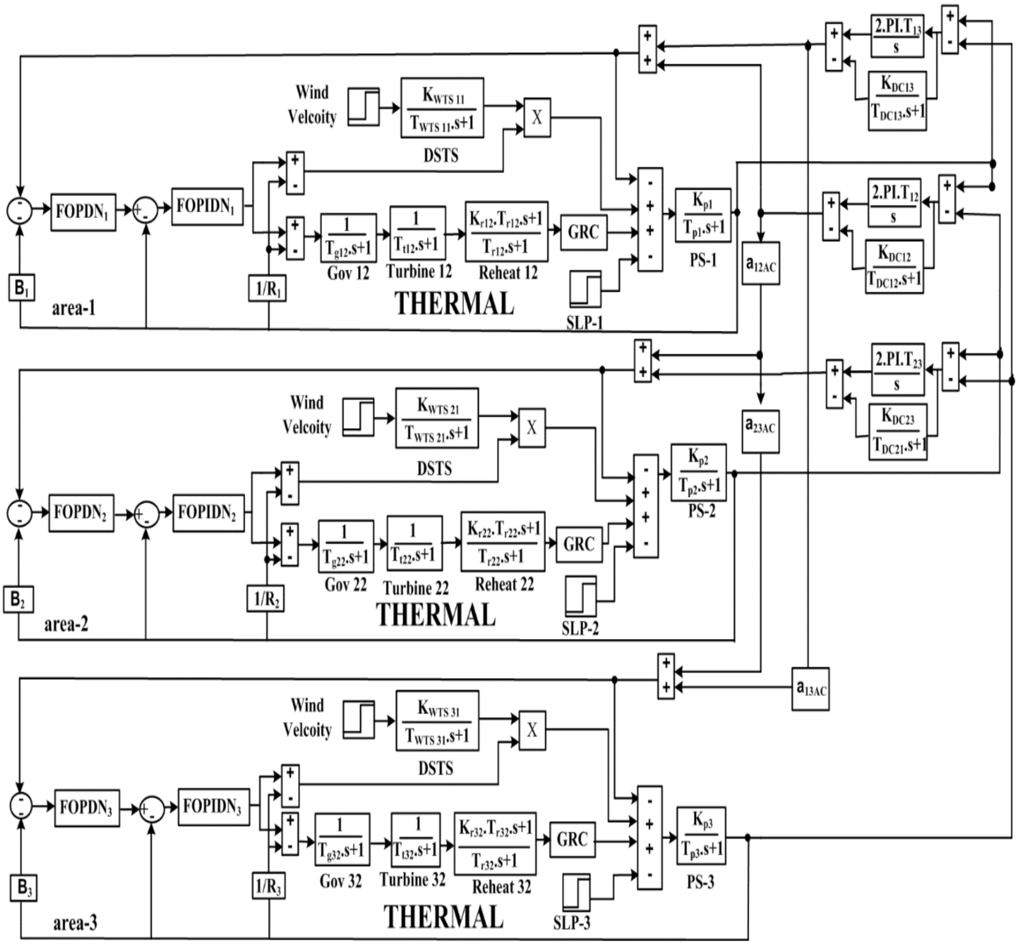

Figure 2: Investigated system

3. Proposed cascade FOPDN-FOPIDN controller

Controller cascading comprises two-loop systems and has more benefits over one-loop systems. The output/primary loop directs the ending output of the systems, while the inner loop is in charge of dampening the influence of the internal process. The cascading structure is in Fig. 3.

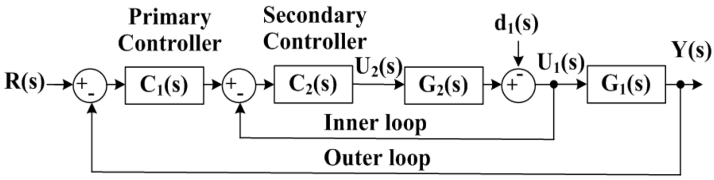

Figure 3: Cascade controller structure

Washima et al. [22, 23] was the first to propose a cascade connection of two FO–FO controllers. Though several P, I and D combinations exist, a unique design of the cascade connection, namely FOPDN-FOPIDN, is suggested with two FO–FO controllers. The TFs of FOPDN-FOPIDN are given by Eqs. (3) and (4).

$$TF_{\text{FOPDN}} = \frac{K_{Pj} + K_{Dj} s^{\mu j} N_j}{\left|1 + N_j / s^{\mu j}\right|}, \tag{3}$$

$$TF_{\text{FOPIDN}} = \frac{K_{Pj} + K_{Ij} / s^{\lambda j} + K_{Dj} s^{\mu j} N_j}{\left|1 + N_j / s^{\mu j}\right|} . \tag{4}$$

The FOPDN controller structure is analogous to the FOPIDN controller structure. The TF model of the FOPDN-FOPIDN controller with AGC as input is in Fig. 4

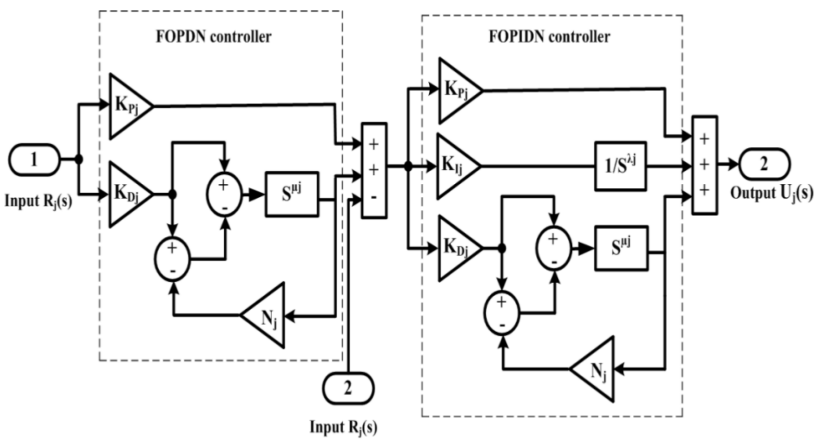

Figure 4: Transfer function model FOPDN-FOPIDN controller

and its gains are optimized by the CSA with constraints in Eq. (5), considering HPA-ISE in Eq. (2).

$$\begin{cases} 0 \leqslant K_{P1j}\,, \quad K_{P2j} \leqslant 1, \quad 0 \leqslant K_{Ij} \leqslant 1, \\ 0 \leqslant K_{D1j}\,, \quad K_{PDj} \leqslant 1, \quad 0 \leqslant \lambda_j\,, \ \ \mu_{1j}, \ \mu_{2j} \leqslant 1, \\ 0 \leqslant N_{1j}\,, \quad N_{2j} \leqslant 100. \end{cases} \tag{5}$$

4. Crow search algorithm

Crows are unique smart entities. It tracks additional birds trying to whack the food. Askarzadeh proposed a revolutionary algorithm named by crow-search algorithm (CSA) considering search agent as a crow [31]. All crows create a flock. Each crow remembers its own hiding places with food and can steal food from another crow. Also, each individual can move randomly with a certain probability.

The position of a crow is described by

$$\mathbf{X}_i^a = \left[X_i^a(1),\ X_i^a(2),\ \ldots,\ X_i^a(d)\right]^T, \tag{6}$$

where: a is crow's number, i is iteration, d is search directions (design variables).

Two path will occur in the each iteration for crow z to follow crow y.

(a) Path 1. The crow a do not take into account position of crow b. The crow y move in direction the best own food place according (7)

$$X_{i+1}^a = X_i^a + r^a f_i^a \left(m_i^b - X_i^a\right) \qquad r_b \geqslant A_i^a\,, \tag{7}$$

where: r^a is the random number, f_i^a is the length of flight. f decides about minima and maxima optimal points, A_i^a is the perceptual probability of crow, m_i^b is the location where individual b have food [34].

(b) Path 2. Knowing crow z approach, crow y sailed to an arbitrary location (8) [35].

$$\mathbf{X}_{i+1}^a = \text{random}\,. \tag{8}$$

After calculation of the positions of all crows in i-th iteration, the matrix m describing the location of food places for each crow is updated.

$$\mathbf{X}_{i+1}^a = \text{random}\,. \tag{9}$$

The fitness of crow's in an iteration is stockpiled and is updated for the subsequent iteration. Figure 5 present the CSA flow chart.

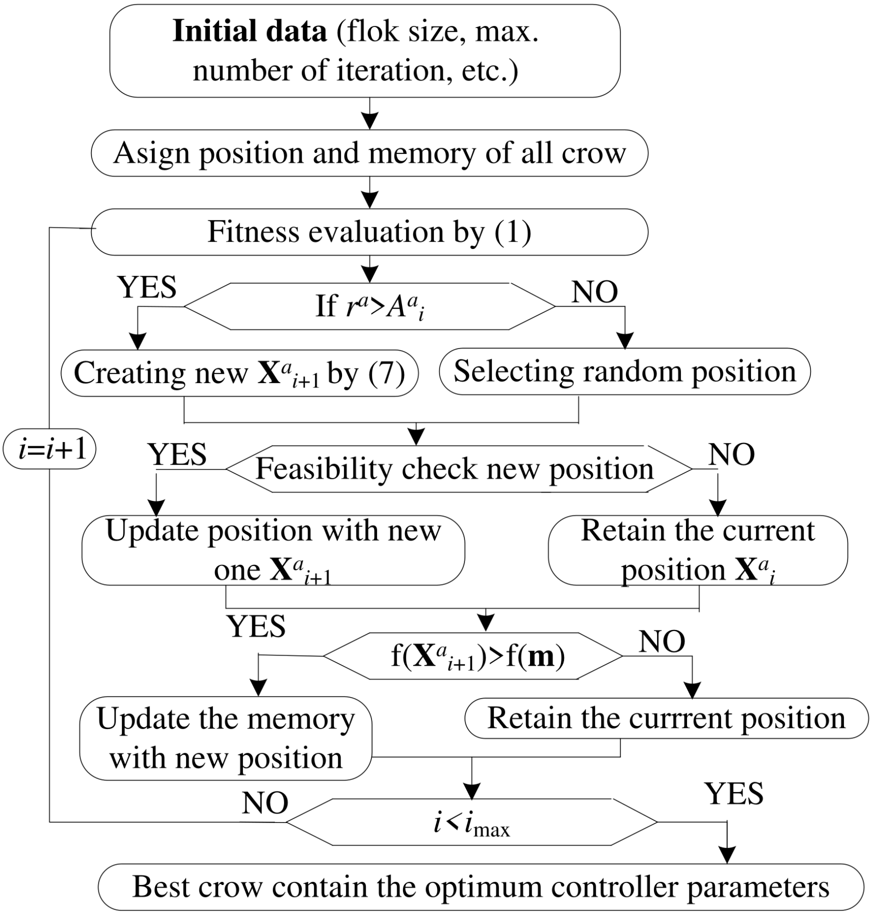

Figure 5: Flow chart of elaborated CSA

5. Results and analysis

The enactment of the AGC scheme encompassing thermal is integrated with DSTS, HVDC is evaluated. The investigations are conceded out with following controllers type: (a) PIDN, (b) TIDN and (c) FOPDN-FOPIDN. Simulations are carried with FOPDN-FOPIDN controller with ODE4 and are optimized by CSA. The optimization simulations were executed for parameters: numbers of crow equal 50, flight length $f = 0.2$, probability $A = 0.1$ and maximum iterations maxiter = 100. Investigated system and controller with optimum parameters are linked with RT-Lab. The obtained responses are compared and validated with RT-Lab Software. The implementation of the AGC model is compiled in RT-Lab and is in Fig. 6.

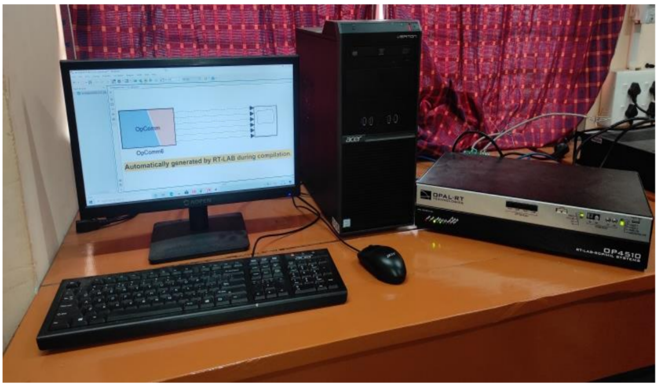

Figure 6: Computer bench with RT-Lab system

5.1. System performance comparison with PIDN, TIDN and FOPDN-FOPIDN in thermal system

The system is presented in Fig. 1(i) is employed with PIDN, TIDN and newly design FOPDN-FOPIDN controllers. Controller limits are enhanced by CSA with HPA-ISE module. of Controller finest values are noted in Table 1 and its consistent responses are in Fig. 7. The value of optimal parameters obtained for the optimization process for the FOPDN-FOPIDN controller are following: $K_{P11} = 0.4673$, $K_{D11} = 0.1899$, $\mu_{I1} = 0.8710$, $N_{11} = 69.943$, $K_{P12} = 0.3862$, $K_{I1} = 0.5881$, $\lambda_1 = 0.8004$, $K_{D12} = 0.1912$, $\mu_{I2} = 0.7820$, $N_{12} = 48.231$, $K_{P21} = 0.6505$, $K_{D21} = 0.3006$, $\mu_{21} = 0.2300$, $N_{21} = 56.704$, $K_{P22} = 0.1506$, $K_{I2} = 0.4009$, $\lambda_2 = 0.4878$, $K_{D22} = 0.7074$, $\mu_{22} = 0.7162$, $N_{22} = 39.256$, $K_{P31} = 0.8773$, $K_{D31} = 0.1367$, $\mu_{31} = 0.4281$, $N_{31} = 87.572$, $K_{P32} = 0.6145$, $K_{I3} = 0.940$, $\lambda_3 = 0.9854$, $K_{D32} = 0.4578$, $\mu_{32} = 0.9178$, $N_{32} = 66.2102$.

Table 1: CSA augmented controller gains of the thermal system considering HPA-ISE

PIDN controller					
	K_{Pj}	K_{Ij}	K_{Dj}	N_j	
Area-1	0.4127	0.583	0.1676	97.4734	
Area-2	0.4008	0.7302	0.5014	9.9626	
Area-3	0.2521	0.0034	0.3271	25.6831	
TIDN controller					
	K_{Tj}	n_j	K_{Ij}	K_{Dj}	N_j
Area-1	0.5980	5.5522	0.2183	0.1301	42.1166
Area-2	0.3606	4.7116	0.6347	0.0068	90.2860
Area-3	0.3738	0.0548	0.4851	0.1333	50.3638

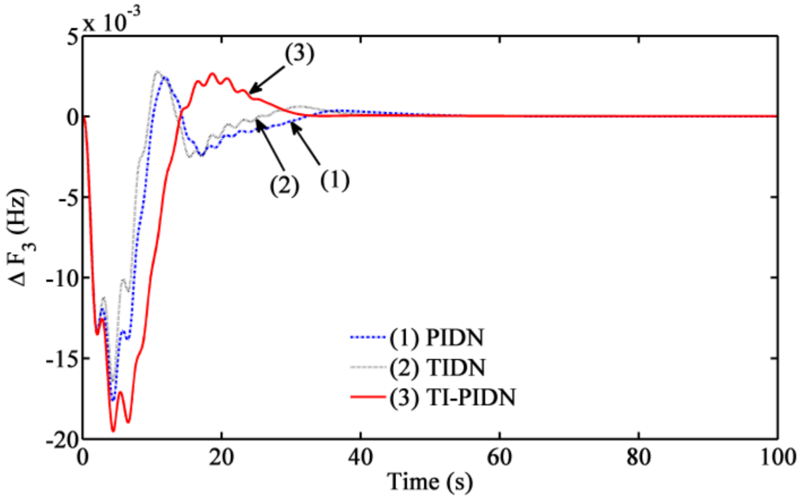

(a)

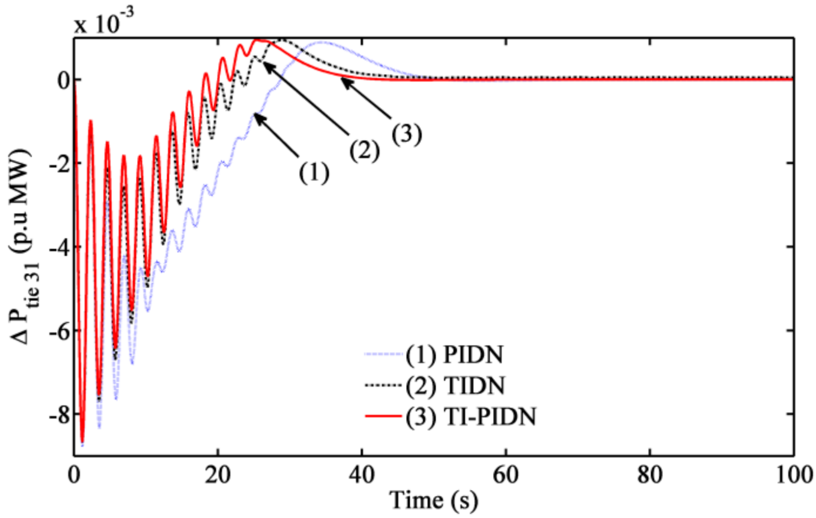

(b)

Figure 7: System dynamic waveforms with thermal system considering MATLAB software (a) ΔF_3, and (b) ΔP_{31}

5.2. Application of RT-Lab software in AGC studies

The system presented in Section-A with CSA optimized FOPDN-FOPIDN controller gains considering MATLAB software are transferred into RT-Lab software. The obtained dynamics using the RT-Lab are compared with MATLAB responses are in Fig. 8.

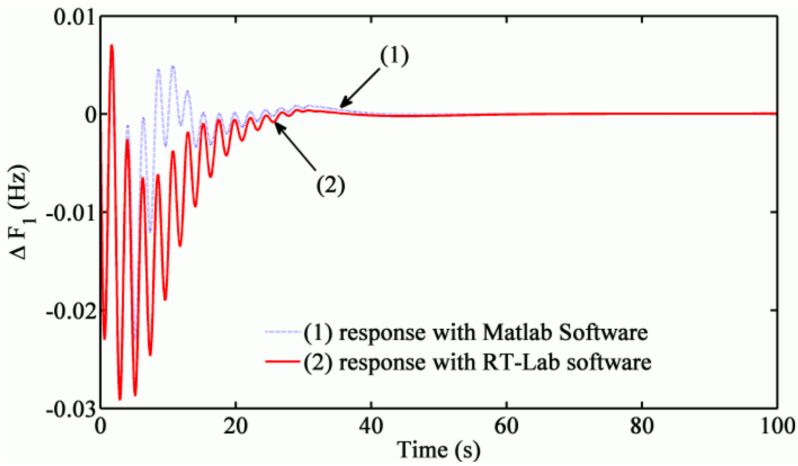

(a)

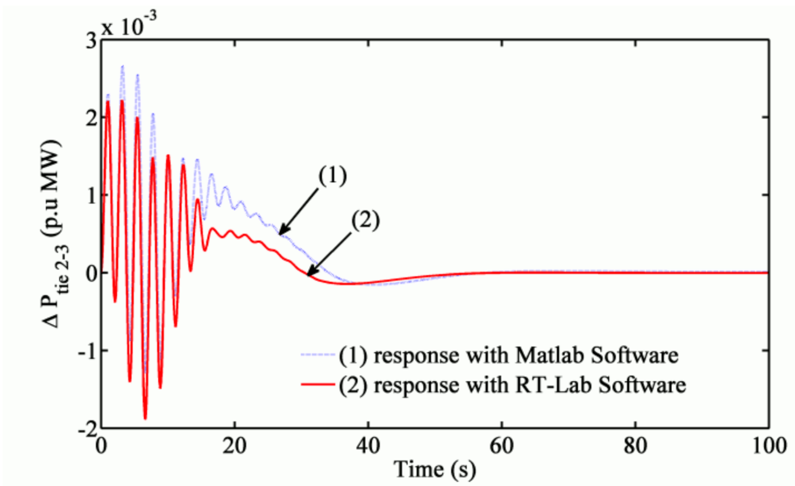

(b)

Figure 8: System dynamic waveforms with thermal system considering MATLAB and RT-Lab software (a) ΔF_3, and (b) ΔP_{31}

It is worth noting that smaller oscillations in the transition state were obtained for the MATLAB environment.

5.3. Comparison of system dynamics among HPA-ISE and ISE with the RT-Lab application

The system presented in Fig. 1 was investigated with the FOPDN-FOPIDN controller and ISE, whose gains were optimized by CSA. The parameters of the controller obtained during optimization process are following: $K_{P11} = 0.8735$,

$K_{D11} = 0.3146$, $\mu_{I1} = 0.8324$, $N_{11} = 33.795$, $K_{P12} = 0.8735$, $K_{I1} = 0.6875$, $\lambda_1 = 0.4354$, $K_{D12} = 0.9379$, $\mu_{I2} = 0.2369$, $N_{12} = 59.870$, $K_{P21} = 0.0720$, $K_{D21} = 0.8703$, $\mu_{21} = 0.3179$, $N_{21} = 37.8461$, $K_{P22} = 0.8706$, $K_{I2} = 0.9254$, $\lambda_2 = 0.9978$, $K_{D22} = 0.4228$, $\mu_{22} = 0.1015$, $N_{22} = 92.340$, $K_{P31} = 0.258$, $K_{D31} = 0.6169$, $\mu_{31} = 0.8914$, $N_{31} = 64.254$, $K_{P32} = 0.8454$, $K_{I3} = 0.7164$, $\lambda_3 = 0.8524$, $K_{D32} = 0.1985$, $\mu_{32} = 0.3321$, $N_{32} = 85.3480$.

The obtained dynamics considering RT-Lab are compared with HPA-ISE and are presented in Fig. 9a and Fig. 9b.

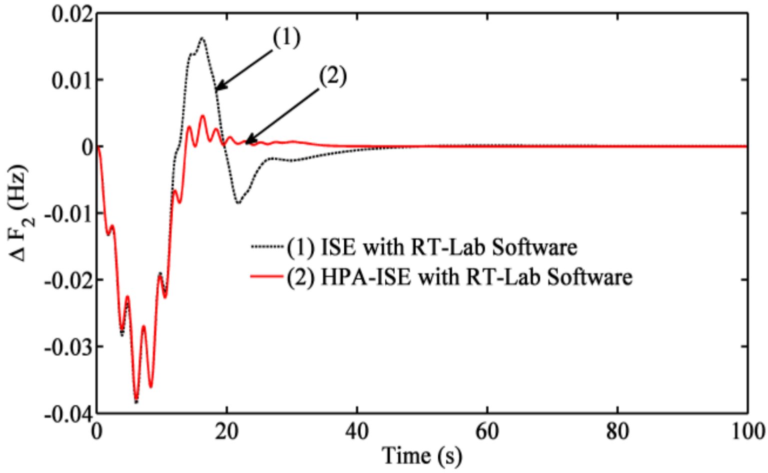

(a)

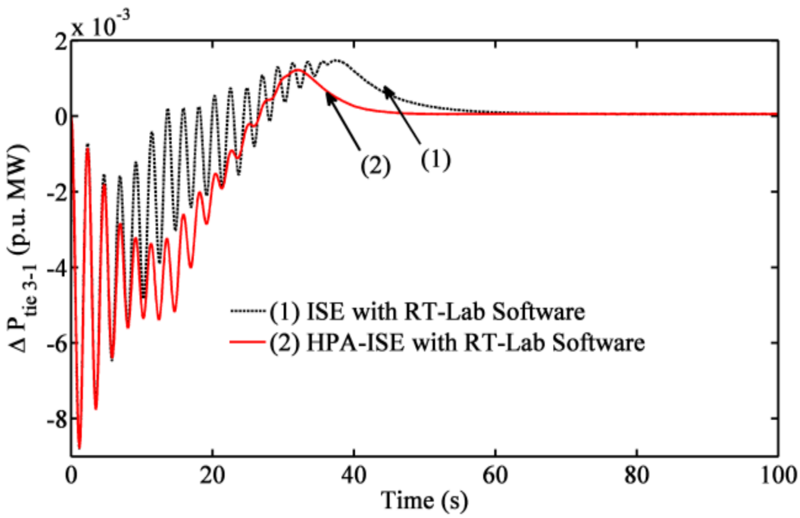

(b)

Figure 9: System dynamics with HPA-ISE and ISE: (a) ΔF_2 and (b) ΔP_{31} in RT-lab

It is noticed that the dynamics with HPA-ISE gives better responses in comparison to ISE. ISE is characterized by high pulsation values in the beginning period.

5.4. Integration of DSTS systems

The system presented in Section 2 was incorporated with DSTS and is shown in Fig. 1(ii). The optimized parameters of FOPDN-FOPIDN with MATLAB have the following values: $K_{P11} = 0.5725$, $K_{D11} = 0.3573$, $\mu_{I1} = 0.5773$, $N_{11} = 0.3623$, $K_{P12} = 0.3967$, $K_{I1} = 0.9328$, $\lambda_1 = 0.7321$, $K_{D12} = 0.7700$, $\mu_{I2} = 0.2217$, $N_{12} = 26.2542$, $K_{P21} = 0.8054$, $K_{D21} = 0.2628$, $\mu_{21} = 0.0677$, $N_{21} = 62.557$, $K_{P22} = 0.1872$, $K_{I2} = 0.7831$, $\lambda_2 = 0.1866$, $K_{D22} = 0.0376$, $\mu_{22} = 0.6490$, $N_{22} = 80.2145$, $K_{P31} = 0.0132$, $K_{D31} = 0.6691$, $\mu_{31} = 0.6925$, $N_{31} = 57.4512$, $K_{P32} = 0.8712$, $K_{I3} = 0.1551$, $\lambda_3 = 0.5721$, $K_{D32} = 0.5964$, $\mu_{32} = 0.7251$, $N_{32} = 15.9802$.

The system dynamics with optimal parameters were matched with the thermal system responses and are shown in Fig. 10a. The obtained dynamics waveform with MATLAB has compared with waveform obtained using RT-Lab software. The comparison is illustrated in Fig. 10b.

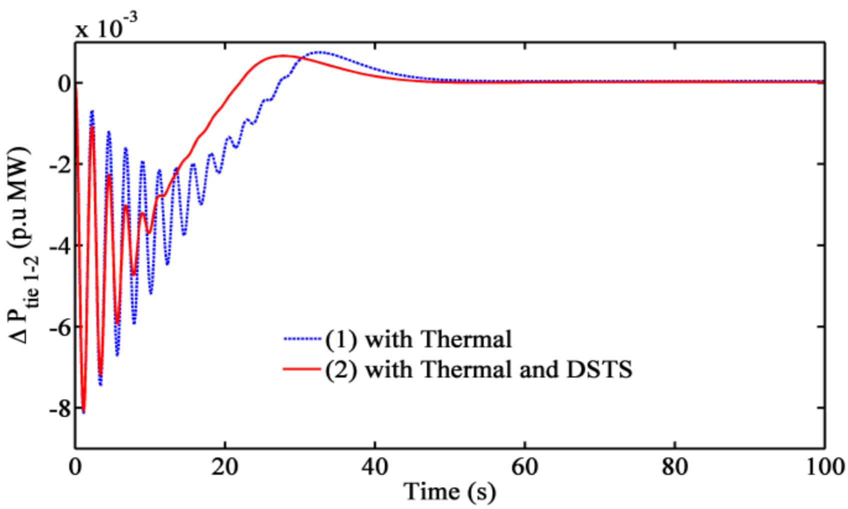

(a)

Figure 10

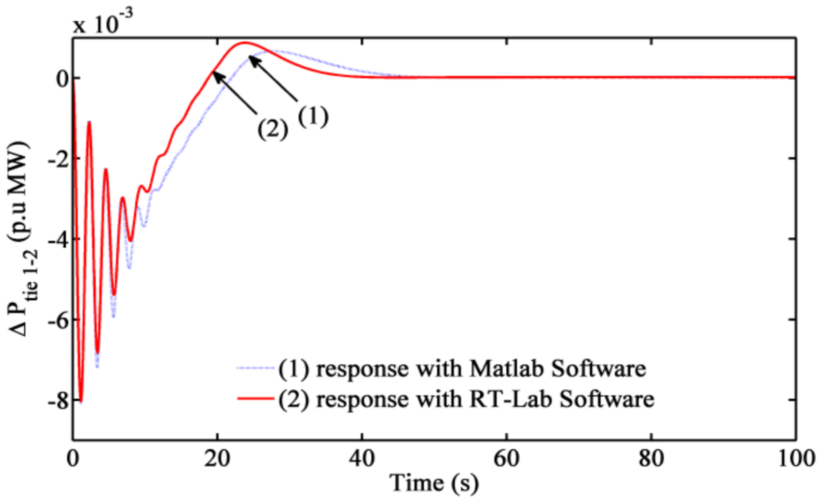

(b)

Figure 10: Dynamics performance compression of system with DSTS integration: (a) ΔP_{12} with MATLAB, and (b) ΔP_{12} with MATLAB and RT-Lab

Figure 10a concludes that the dynamics with DSTS integration provides better responses. In addition, responses in Fig. 10b with RT-Lab shows improved responses.

5.5. Integration of HVDC system

DSTS-thermal system in Section-D is linked with HVDC. Figure 1(iii) illustrates the investigated system. The CSA is used to optimize FOPDN-FOPIDN parameters. The optimized parameters of FOPDN-FOPIDN with MATLAB have the following values: $K_{P11} = 0.6554$, $K_{D11} = 0.7111$, $\mu_{I1} = 0.7060$, $N_{11} = 0.3183$, $K_{P12} = 0.2769$, $K_{I1} = 0.0461$, $\lambda_1 = 0.9131$, $K_{D12} = 0.8234$, $\mu_{I2} = 0.5946$, $N_{12} = 22.2145$, $K_{P21} = 0.4446$, $K_{D21} = 0.0254$, $\mu_{21} = 0.7099$, $N_{21} = 22.496$, $K_{P22} = 0.6478$, $K_{I2} = 0.0415$, $\lambda_2 = 0.4723$, $K_{D22} = 0.0563$, $\mu_{22} = 0.1744$, $N_{22} = 67.452$, $K_{P31} = 0.8175$, $K_{D31} = 0.3115$, $\mu_{31} = 0.2413$, $N_{31} = 10.9647$, $K_{P32} = 0.3141$, $K_{I3} = 0.9047$, $\lambda_3 = 0.7496$, $K_{D32} = 0.4864$, $\mu_{32} = 0.7521$, $N_{32} = 27.8941$.

The transients with HVDC integration are in Fig. 11a. The comparative dynamics with MATLAB and RT Lab are in Fig. 11b.

From Fig. 11 it is observed that responses with RT Lab software provide better dynamics.

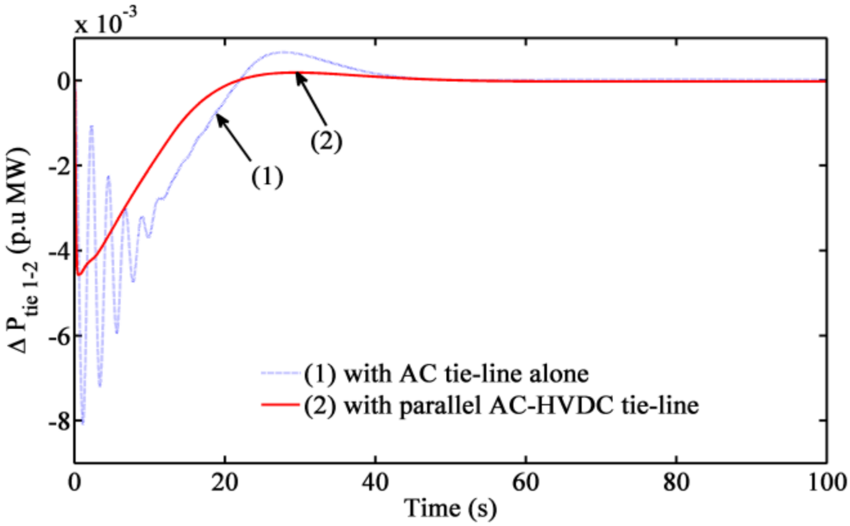

(a)

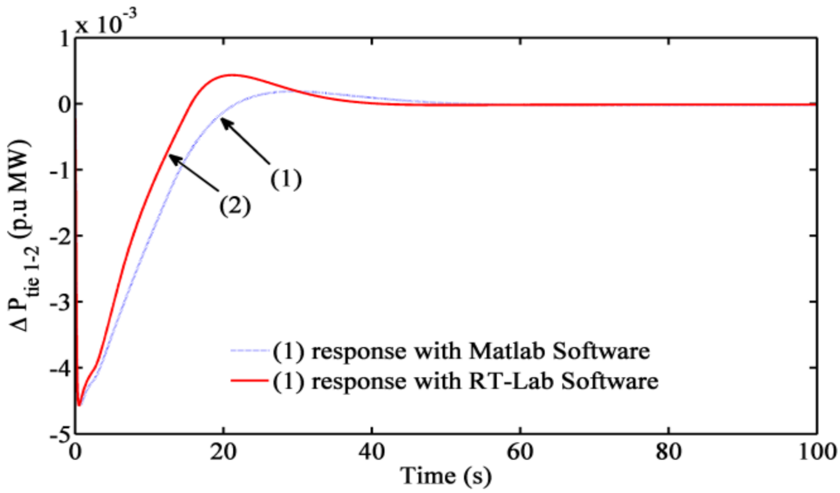

(b)

Figure 11: System dynamics with AC-HVDC: (a) ΔF_1, with MATLAB and (b) ΔF_1 with MATLAB and RT-Lab

5.6. Sensitivity analysis of the thermal-DSTS system with FOPDN-FOPIDN controller

The system presented in Fig. 2 is exposed to deviations in loading conditions (LC) i.e., (±15%). Simulations were passed in RT Lab software with FOPDN-FOPIDN controller and responses are in Fig. 12.

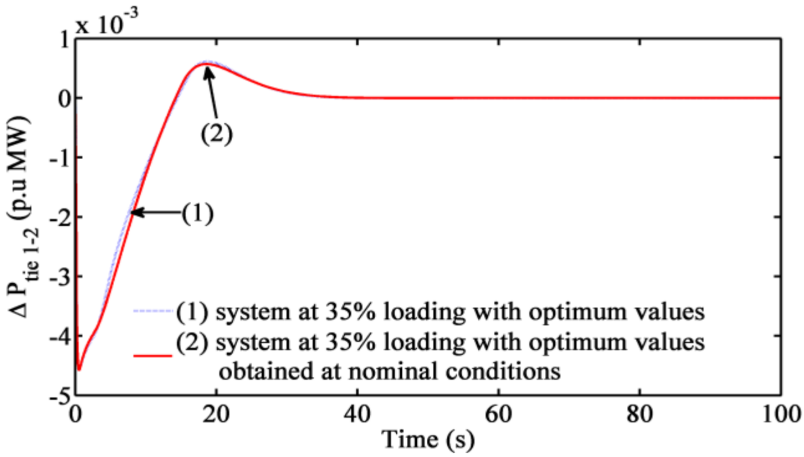

(a)

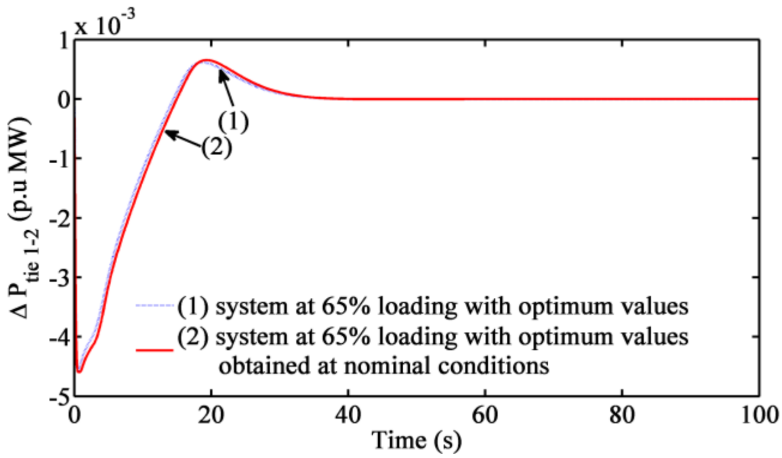

(b)

Figure 12: System condition with deviations in LC (±15%): (a) ΔF_1 and (b) ΔP_{12} with RT-Lab

6. Conclusions

The application of RT-Lab software in AGC studies has been successfully adopted. A new PI named by HPA-ISE is applied in AGC studies. A new control design named by the FOPDN-FOPIDN controller was investigated and its parameters were enhanced by the crow search algorithm. The performance of FOPDN-FOPIDN outperforms over TIDN and PIDN controller. The system dynamics response with HPA-USE has better performance reliability in comparison to ISE. It is to point out, also that better thermal response is obtained by incorporation of DSTS. Additionally, it has been noted that the connection of HVDC with the AC system can enhance system dynamics. Besides, a deviation in LC through SA recommends that the proposed FOPDN-FOPIDN controller is vigorous. In addition, RT-Lab software validates the system dynamics obtained with MATLAB and is obvious that responses with RT-Lab outperforms over MATLAB software.

Nomenclature

F	frequency (Hz)
P_{tie}	tie-power
SLP	step load perturbation
AGC	automatic generation control
DSTS	dish-stirling solar thermal system
HVDC	high voltage direct current
KP, KI, KD	proportional, integral and derivative gains
λ, μ	proportional and integral non-integer parameters
CSA	crow search algorithm
MATLAB	matrix laboratory
RT-Lab	real time laboratory
RES	renewable energy source
HPA	hybrid peak area
ISE	integral squared error
LC	loading condition
SA	sensitivity analysis

References

[1] O.I. Elgerd: *Electric Energy Systems Theory: An Introduction*. New Delhi, Tata McGraw-Hill, 2007.

[2] P. Kundur: *Power System Stability and Control*. New Delhi, Tata McGraw Hill, 1993.

[3] H. Golpira, H. Bevrani and H. Golpira: Application of GA optimization for automatic generation control design in an interconnected power system. *Energy Conversion and Management*, **52**(5), (2011), 2247–2255. DOI: 10.1016/j.enconman.2011.01.010.

[4] J. Nanda, A. Mangla and S. Suri: Some new findings on automatic generation control of an interconnected hydrothermal system with conventional controllers. *IEEE Transactions on Energy Conversion*, **21**(1), (2006), 187–194. DOI: 10.1109/TEC.2005.853757.

[5] J. Morsali, K. Zare and M.T. Hagh: Applying fractional order PID to design TCSC-based damping controller in coordination with automatic generation control of interconnected multi-source power system. *International Journal Engineering Science and Technology*, **20**(1), (2017), 1–17. DOI: 10.1016/j.jestch.2016.06.002.

[6] H. Bevrani. A. Ghosh and G. Ledwich: Renewable energy sources and frequency regulation: survey and new perspectives. *IET Renewable Power Generation*, **4**(5), (2010), 438–457. DOI: 10.1049/iet-rpg.2009.0049.

[7] D.C. Das, N. Sinha and A.K. Roy: GA based frequency controller for solar thermal–diesel–wind hybrid energy generation/energy storage system. *International Journal of Electrical Power and Energy Systems*, **43**(1), (2012), 62–79. DOI: 10.1016/j.ijepes.2012.05.025.

[8] A. Rahman, L.C. Saikia and N. Sinha: AGC of dish-Stirling solar thermal integrated thermal system with biogeography based optimized three degree of freedom PID controller. *IET Renewable Power Generation*, **10**(8), (2016), 1161–1170. DOI: 10.1049/iet-rpg.2015.0474.

[9] A. Rahman, L.C. Saikia and N. Sinha: Automatic generation control of an interconnected two-area hybrid thermal system considering dish-Stirling solar thermal and wind turbine system. *IET Renewable Power Generation*, **10**(8), (2017), 41–54. DOI: 10.1016/j.renene.2016.12.048.

[10] A. Sahan and L.C. Saikia: Utilization of ultra-capacitor in load frequency control under restructured STPP-thermal power systems using WOA optimized PIDN-FOPD controller. *IET Generation, Transmission and Distribution*, **11**(13), (2017) 3318–3331. DOI: 10.1049/iet-gtd.2017.0083.

[11] W. Tasnin and L.C. Saikia: Maiden application of an sine–cosine algorithm optimised FO cascade controller in automatic generation control of multi-area thermal system incorporating dish-Stirling solar and geothermal power plants. *IET Renewable Power Generation*, **12**(5), (2018), 585–597. DOI: 10.1049/iet-rpg.2017.0063.

[12] S. Wang, L. Zhao and L. Zhou: A control method of fault current in MT-HVDC grid based on current limiter and circuit breaker. *Archives of Electrical Engineering*, **70**(4), (2021), 907–923. DOI: 10.24425/aee.2021.138269.

[13] O.D. Adeuyi, M. Cheah-Mane, J. Liang, N. Jenkins, Y. Wu, C. Li and X. Wu: Frequency support from modular multilevel converter based multi-

terminal HVDC schemes. *IEEE Power and Energy Society General Meeting*, Denver, United States, (2015). DOI: 10.1109/PESGM.2015.7286086.

[14] E. Rakhshani and P. Rodriguez: Inertia emulation in AC/DC interconnected power systems using derivative technique considering frequency measurement effects. *IEEE Transactions on Power Systems*, **32**(5), (2017), 3338–3351. DOI: 10.1109/TPWRS.2016.2644698.

[15] S. Singh and I. Nasiruddin: Optimal AGC regulator for multi-area interconnected power systems with parallel AC/DC links. *Cogent Engineering Journal*, **3**(1), (2016). DOI: 10.1080/23311916.2016.1209272.

[16] G. Sharma, I. Nasiruddin, K.R. Niazi and R.C. Bansal: Adaptive fuzzy critic based control design for AGC of power system connected via AC/DC tie-lines. *IET Generation, Transmission and Distribution*, **11**(2), (2016), 560–569. DOI: 10.1049/iet-gtd.2016.1164.

[17] B. Uzunoğlu: An adaptive bayesian approach with subjective logic reliability networks for preventive maintenance. *IEEE Transactions on Reliability*, **69**(3), (2020), 916–924. DOI: 10.1109/TR.2019.2916722.

[18] N. Pathak, A. Verma, T.S. Bhatti and I. Nasiruddin: Modeling of HVDC tie-links and their utilization in AGC/LFC operations of multi-area power systems. *IEEE Transactions on Industrial Electronics*, **66**(3), (2019). 2185–2197. DOI: 10.1109/TIE.2018.2835387.

[19] K. Jagatheesan, B. Anand, S. Samanta, N. Dey, A.S. Ashour and V.E. Balas: Design of a proportional-integral-derivative controller for an automatic generation control of multi-area power thermal systems using firefly algorithm. *IEEE/CAA Journal of Automatica Sinica*, **6**(2), (2019), 503–515. DOI: 10.1109/JAS.2017.7510436.

[20] I. Pan and S. Das: Fractional order AGC for distributed energy resources using robust optimization. *IEEE Transactions on Smart Grid*, **7**(5), (2016), 2175–2186. DOI: 10.1109/TSG.2015.2459766.

[21] P.N. Topno and S. Chanana: Tilt integral derivative control for two-area load frequency control problem. *2nd International Conference on Recent Advances in Engineering and Computational Sciences*, Chandigarh, India, (2015). DOI: 10.1109/RAECS.2015.7453361.

[22] W. Tasnin and L.C. Saikia: Performance comparison of several energy storage devices in deregulated AGC of a multi-area system incorporating geothermal power plant. *IET Renewable Power Generation*, **12**(7), (2018), 761–772. DOI: 10.1049/iet-rpg.2017.0582.

[23] W. Tasnin, L.C. Saikia and M. Raju: Deregulated AGC of multi-area system incorporating dish-Stirling solar thermal and geothermal power plants

using fractional order cascade controller. *IET Generation, Transmission and Distribution*, **101** (2018), 60–74. DOI: 10.1016/j.ijepes.2018.03.015.

[24] K. Bentata, A. Mohammedi and T. Benslimane: Development of rapid and reliable cuckoo search algorithm for global maximum power point tracking of solar PV systems in partial shading condition. *Archives of Control Sciences*, **31**(3), (2021), 495–526. DOI: 10.24425/acs.2021.138690.

[25] D.K. Dash, P.K. Sadhu and B. Subudhi: Spider monkey optimization (SMO) – lattice Levenberg–Marquardt recursive least squares based grid synchronization control scheme for a three-phase PV system. *Archives of Control Sciences*, **31**(3), (2021), 707–730. DOI: 10.24425/acs.2021.138698.

[26] R. Devarapalli and V. Kumar: Power system oscillation damping controller design: a novel approach of integrated HHO-PSO algorithm. *Archives of Control Sciences*, **31**(3), (2021), 553–591. DOI: 10.24425/acs.2021.138692.

[27] A. Rahman, L.C. Saikia and N. Sinha: Load frequency control of a hydro-thermal system under deregulated environment using biogeography-based optimised three-degree-of freedom integral derivative controller. *IET Generation, Transmission and Distribution*, **9**(15), (2015), 2284–2293. DOI: 10.1049/iet-gtd.2015.0317.

[28] J. Pierezan and L. Dos Santos Coelho: Coyote optimization algorithm: A new metaheuristic for global optimization problems. *IEEE Congress on Evolutionary Computation*, Rio de Janeiro, Brazil, (2018). DOI: 10.1109/CEC.2018.8477769.

[29] Ko-Wei Huang and Wu Ze-Xue: CPO: A crow particle optimization algorithm. *International Journal of Computational Intelligence Systems*, **12**(1), (2018), 426–435. DOI: 10.2991/ijcis.2018.125905658.

[30] N.R. Babu and L.C. Saikia: Automatic generation control of a solar thermal and dish-Stirling solar thermal system integrated multi-area system incorporating accurate HVDC link model using crow search algorithm optimised FOPI Minus Minus FODF controller. *IET Renewable Power Generation*, **13**(12), (2019), 2221–2231. DOI: 10.1049/iet-rpg.2018.6089.

[31] A. Askarzadeh: A novel metaheuristic method for solving constrained engineering optimization problems: Crow search algorithm. *Journal of Computers and Structures*, **169** (2016), 1–12. DOI: 10.1016/j.compstruc.2016.03.001.

[32] N. Pathak and Z. Hu: Hybrid-peak-area-based performance index criteria for AGC of multi-area power systems. *IEEE Transactions on Industrial Informatics*, **15**(11), (2019), 5792–5802. DOI: 10.1109/TII.2019.2905851.

[33] A. Ali, J. Chuanwen, M.M. Khan, S. Habib and Y. Ali: Performance evaluation of ZVS/ZCS high efficiency AC/DC converter for high power applications. *Bulletin of the Polish Academy of Sciences Technical Sciences*, **68**(4), (2020), 793–807. DOI: 10.24425/bpasts.2020.134185.

[34] N. Amor, M. Tayyab Noman, M. Petru, A. Mahmood and A. Ismail: Neural network-crow search model for the prediction of functional properties of nano TiO2 coated cotton composites. *Scientific Reports*, **11** Article number: 13649, (2021). DOI: 10.1038/s41598-021-93108-9.

[35] M. Djurdjev, R. Cep, D. Lukic, A. Antic, B. Popovic and M. Milosevic: A genetic crow search algorithm for optimization of operation sequencing in process planning. *Applied Sciences*, **11**(5), (2021). DOI: 10.3390/app11051981.